Biochemical and Biophysical Research Communications 439 (2013) 291–296

Contents lists available at ScienceDirect

Biochemical and Biophysical Research Communications

journal homepage: www.elsevier.com/locate/ybbrc

Breast cancer cell behaviors on staged tumorigenesis-mimicking matrices derived from tumor cells at various malignant stages

Takashi Hoshiba [a,b], Masaru Tanaka [a,*]

[a] Graduate School of Science and Engineering, Yamagata University, 4-3-16 Jonan, Yonezawa, Yamagata 992-8510, Japan
[b] International Center for Materials Nanoarchitectonics (MANA), National Institute for Materials Science, 1-1 Namiki, Tsukuba, Ibaraki 305-0044, Japan

ARTICLE INFO

Article history:
Received 5 August 2013
Available online 23 August 2013

Keywords:
Tumor
Extracellular matrix
Tumor malignancy
Cell proliferation
Chemoresistance
Decellularization

ABSTRACT

Extracellular matrix (ECM) has been focused to understand tumor progression in addition to the genetic mutation of cancer cells. Here, we prepared "staged tumorigenesis-mimicking matrices" which mimic *in vivo* ECM in tumor tissue at each malignant stage to understand the roles of ECM in tumor progression. Breast tumor cells, MDA-MB-231 (invasive), MCF-7 (non-invasive), and MCF-10A (benign) cells, were cultured to form their own ECM beneath the cells and formed ECM was prepared as staged tumorigenesis-mimicking matrices by decellularization treatment. Cells showed weak attachment on the matrices derived from MDA-MB-231 cancer cells. The proliferations of MDA-MB-231 and MCF-7 was promoted on the matrices derived from MDA-MB-231 cancer cells whereas MCF-10A cell proliferation was not promoted. MCF-10A cell proliferation was promoted on the matrices derived from MCF-10A cells. Chemoresistance of MDA-MB-231 cells against 5-fluorouracil increased on only matrices derived from MDA-MB-231 cells. Our results showed that the cells showed different behaviors on staged tumorigenesis-mimicking matrices according to the malignancy of cell sources for ECM preparation. Therefore, staged tumorigenesis-mimicking matrices might be a useful *in vitro* ECM models to investigate the roles of ECM in tumor progression.

1. Introduction

Cancer originates from genetic mutations that alter cellular functions such as proliferation and survival, thereby leading to uncontrolled cell proliferation [1]. Decades of research have revealed the effects caused by these genetic mutations. Recent studies have also focused on the roles of the extracellular microenvironment of tumor tissues in tumor progression [2,3]. The effects of the tumor extracellular microenvironment are reflected in the architecture of the tumor tissue, which differs radically from that of normal tissue [4]. The extracellular matrix (ECM), a key component of the tumor tissue microenvironment, regulates diverse cellular functions such as cell attachment, survival, and proliferation [5]. It is well established that the ECM is dynamically remodeled during tumor progression. For example, the levels of tenascin-C, periostin, and fibronectin increase in the ECM of breast cancer with poor prognosis [4,6]. Laminins also increase in the ECM in breast cancer, particularly in cases of metastatic cancer [7,8]. These findings strongly support that ECM remodeling in the tumor tissue plays an important role in tumor progression. Many studies have been conducted to identify the components of the ECM in tumor tissue during tumor progression to improve the prediction of tumor prognosis [4–8]. Additionally, the functions of each ECM protein have been well studied using specific gene knocked-down models and isolated ECM protein-coated substrates for the *in vitro* culture of tumor cell lines with different metastatic potential [9,10]. However, few studies have addressed the comprehensive influence of the ECM as an assembled structure on tumor progression. Therefore, we reasoned that the *in vitro* tumor ECM model at distinct stages of malignancy should provide valuable insights into the roles of the tumor ECM on tumor progression.

Decellularized matrices have been widely used to generate *in vitro* models of the ECM [11,12]. We have previously reported on *in vitro* ECM models mimicking the *in vivo* ECM of differentiating tissues during the osteogenesis and adipogenesis of mesenchymal stem cells (MSCs) [13–16]. These stepwise tissue-development-mimicking matrices were formed by culturing MSCs and controlling their developmental stages, and the resulting matrices were prepared as new cell culture substrates by the decellularization technique. We demonstrated that the differentiation balance of MSCs between osteogenesis and adipogenesis can be regulated by stepwise tissue-development-mimicking matrices through the control of intracellular signals and transcription factor expression [13–16]. These findings revealed the potential of stepwise tissue-development-mimicking matrices to provide useful

* Corresponding author.
E-mail address: tanaka@yz.yamagata-u.ac.jp (M. Tanaka).

0006-291X/$ - see front matter © 2013 Elsevier Inc. All rights reserved.
http://dx.doi.org/10.1016/j.bbrc.2013.08.038

in vitro models to study the role of the ECM in stem cell differentiation.

In the present study, our goal was to generate "staged tumorigenesis-mimicking matrices" that mimic the ECM of *in vivo* tumor tissues at different malignant stages as a new *in vitro* ECM model representing the remodeled ECM during tumor progression in a similar fashion. We also observed the tumor cell phenotypes on these matrices for the analysis of the role of ECM remodeling in tumor progression. Specifically, we focused on breast tumor progression using the MDA-MB-231 and MCF-7 breast cancer cell lines, which differ in their invasive properties, and compared them to a breast-benign cell line, MCF-10A cells, derived from a benign mammary gland. A summary of the cell properties for the preparation of the staged tumorigenesis-mimicking matrices is shown in Table S1.

2. Materials and methods

2.1. Cell culture

The human invasive breast cancer cell line MDA-MB-231 (American Type Culture Collection (ATCC), Manassas, VA) and the human mammary gland benign cell line MCF-10A (ATCC) were cultured at a density of 10,000 cells/cm^2 on tissue culture polystyrene (TCPS) plates for 1 week in Dulbecco's modified Eagle/Nutrient Mixture F-12 (basal DMEM/F-12, Gibco, Carlsbad, CA) containing 10% fetal bovine serum (FBS, Equitech-Bio, Kerrville, TX) (serum DMEM/F-12). Additionally, the human non-invasive breast cancer cell line MCF-7 (Health Science Research Resources Bank, Osaka, Japan) was cultured at a density of 30,000 cells/cm^2 on TCPS plates for 1 week in serum DMEM/F-12. Summary of matrices preparation conditions is shown in Table S1.

2.2. Semi-quantitative reverse transcription-polymerase chain reaction (RT-PCR)

Total RNA was extracted from the cells under the conditions mentioned above using Sepasol-RNA I Super reagent according to the manufacturer's instructions (Nacalai Tesque, Kyoto, Japan). Total RNA (1 μg) was used as a first-strand reaction that included random hexamer primers and ReverTra Ace-α reverse transcriptase (TOYOBO, Osaka, Japan). Semi-quantitative RT-PCR was performed using HybriPol DNA polymerase (Nippon Genetics, Tokyo, Japan) with specific human primer sets, as shown in Table 1. All primers were obtained from Nihon Gene Research Laboratories (Sendai, Japan). For each experiment, *GAPDH* was amplified to normalize the expression of the other genes in the sample. The PCR products were analyzed by 1% agarose gel electrophoresis.

Table 1
Primers for semi-quantitative RT-PCR analysis.

mRNA		Oligonucleotide
GAPDH	Forward	5′-GGGCTGCTTTTAACTCTGGT-3′
	Reverse	5′-TGGCAGGTTTTTCTAGACGG-3′
LAMA3	Forward	5′-GACCCTTGACCCCCACAAT-3′
	Reverse	5′-GCTCGTACTGCATGTCCCCT-3′
LAMA5	Forward	5′-AGTCGATACAGACACCCCCA-3′
	Reverse	5′-AGTCGATACAGACACCCCCA-3′
FN1	Forward	5′-ACCAATGCCAGGATTCAGAG-3′
	Reverse	5′-ATACCACACCAGGCTTCAGG-3′
TNC	Forward	5′-GATGAAGGGGTCTTCGACAA-3′
	Reverse	5′-AATCCGGAAGCTCTCCACTT-3′
POSTN	Forward	5′-GGGACTAACTGCAACGGAGA-3′
	Reverse	5′-ATGCCCAGAGTGCCATAAAC-3′

GAPDH was designed according to Tuli et al. [17]. *LAMA3*, *LAMA5*, *FN1*, *TNC*, and *POSTN* were designed by our laboratory.

2.3. Preparation of staged tumorigenesis-mimicking matrices

Staged tumorigenesis-mimicking matrices were prepared using a method similar to that reported previously [13,15,16]. Briefly, after culture for 1 week on TCPS in serum DMEM/F-12, the cellular components were removed from the matrices through incubation with phosphate-buffered saline (PBS) containing 0.5% Triton X-100 and 20 mM NH_4OH for 5 min at 37 °C. Subsequently, the samples were treated with 100 μg/ml DNase I (Roche Applied Science, Penzberg, Germany) and 100 μg/ml RNase A (Nacalai Tesque) for 1 h at 37 °C. After the cellular components were removed, the matrices were treated with 0.1% glutaraldehyde in PBS for 6 h at 4 °C to stabilize the matrices, and they were then treated with 0.1 M glycine in PBS. Additionally, bovine fibronectin-(FN, Calbiochem, Darmstadt, Germany) and bovine serum albumin-(BSA, Sigma, St Louis, MO) coated TCPSs were prepared. For the preparation of these protein-coated TCPSs, 10 μg/ml FN and 10 mg/ml BSA in PBS were added to the plates and the plates were incubated at 37 °C for 4 and 2 h, respectively. After coating, the plates were washed with water and then air-dried for 1 h.

2.4. Confirmation of decellularization

After culturing the cells for matrix preparation, the cells were fixed with 0.1% glutaraldehyde for 6 h at 4 °C and then treated with 0.1 M glycine in PBS. After fixation, the cells were permeabilized by treatment with 0.2% Triton X-100 in PBS for 2 min. To visualize the cell nuclei, the cells and the staged tumorigenesis-mimicking matrices were stained with 10 μg/ml Hoechst 33258 (Wako) for 15 min at room temperature. To visualize the actin fibers, the cells and staged tumorigenesis-mimicking matrices were incubated with Alexa 488-conjugated phalloidin (Invitrogen, Carlsbad, CA) for 1 h at room temperature. The cells and matrices were then observed under a fluorescence microscope. The results were shown in pseudo-color mode using Adobe Photoshop 6.0. To visualize whole proteins in the matrices, coomassie brilliant blue (CBB) staining (Nacalai Tesque) was performed.

2.5. Cell attachment assay

MDA-MB-231, MCF-7, and MCF-10A cells were seeded on staged tumorigenesis-mimicking matrices as well as FN- and BSA-coated TCPSs and bare TCPS plates in basal DMEM/F-12 at a density of 10,000 cells/cm^2. After 1 h incubation, the non-attached cells were removed from the culture by washing with PBS twice, and then the attached cells were fixed with 0.1% glutaraldehyde overnight at room temperature. To visualize the cells, the cells were stained with 0.2% crystal violet (Wako, Osaka, Japan) solution for 15 min. After the staining, the attached cells in three randomly selected fields were counted using an optical microscope.

2.6. Cell proliferation assay

For the proliferation assays of MDA-MB-231, MCF-7, and MCF-10A cells, the cells were seeded on the staged tumorigenesis-mimicking matrices, FN-coated TCPS, and bare TCPS at a density of 5000 cells/cm^2 in serum DMEM/F-12. After 1, 2, and 3 days of culture, the cell number was quantified by a colorimetric WST-8 assay (Dojindo Laboratories, Kumamoto, Japan).

2.7. Cytotoxicity of anti-cancer drugs

MDA-MB-231 cells were seeded on staged tumorigenesis-mimicking matrices, FN-coated TCPS, and bare TCPS at a density of 30,000 cells/cm^2. After 1 day of culture in serum DMEM/F-12, the media were changed to serum DMEM/F-12 supplemented with 5-fluorouracil (5-FU, Sigma) or doxorubicin (Dox, Wako) at the indicated concentrations. After an additional 3 days of culture, the viable cells were evaluated by the WST-8 assay. The data are expressed as the percentage of viable cells relative to those without anti-cancer drugs.

2.8. Statistical analysis

All data are represented as the means ± SD (n = 3). All statistical analyses were performed using *R*, a language and environment for statistical computing. Significant differences were statistically detected by analysis of variance. The Tukey multiple comparison test was applied as a post hoc test. P values of <0.05 were considered to be statistically significant.

3. Results and discussion

3.1. ECM expression pattern

First, we compared the ECM gene expression patterns among MDA-MB-231, MCF-7, and MCF-10A cells (Fig. 1A). *LAMA3* was strongly expressed in MDA-MB-231 cells, which is consistent with previous report [7]. The *LAMA5* expression levels in MDA-MB-231 and MCF-7 cells were higher than in MCF-10A cells. *FN1*, *TNC*, and *POSTN* were strongly expressed in MCF-10A cells. *FN1* and *TNC* were moderately expressed in MDA-MB-231 cells. These results are coincident with previous report [18]. These results indicate that the ECM expression patterns are different among tumor cells at different malignant stages.

Generally, in breast cancer tissues, fibronectin, tenascin-C, and periostin are observed in accordance with the cancer progression [4,6]. On the other hand, these genes expression levels were highest in MCF-10A cells. MCF-10A cells are derived from benign fibrocystic breast tissue [19]. The cells in benign fibrocystic breast tissue can express *TNC* [20]. Therefore, *TNC* expression was observed in MCF-10A cells. Additionally, the MCF-10A cells derived from benign fibrocystic breast tissue had high expression of *FN1* and *POSTN*. Moreover, it has been reported that tenascin-C in breast cancer tissue is produced by myofibroblasts that neighbor the cancer cells [21]. Therefore, little or no *TNC* expression was observed in MDA-MB-231 and MCF-7 cells.

3.2. Preparation of staged tumorigenesis-mimicking matrices by decellularization

To apply the ECM proteins that are deposited by these cells as new cell culture substrates, we next attempted to remove cellular

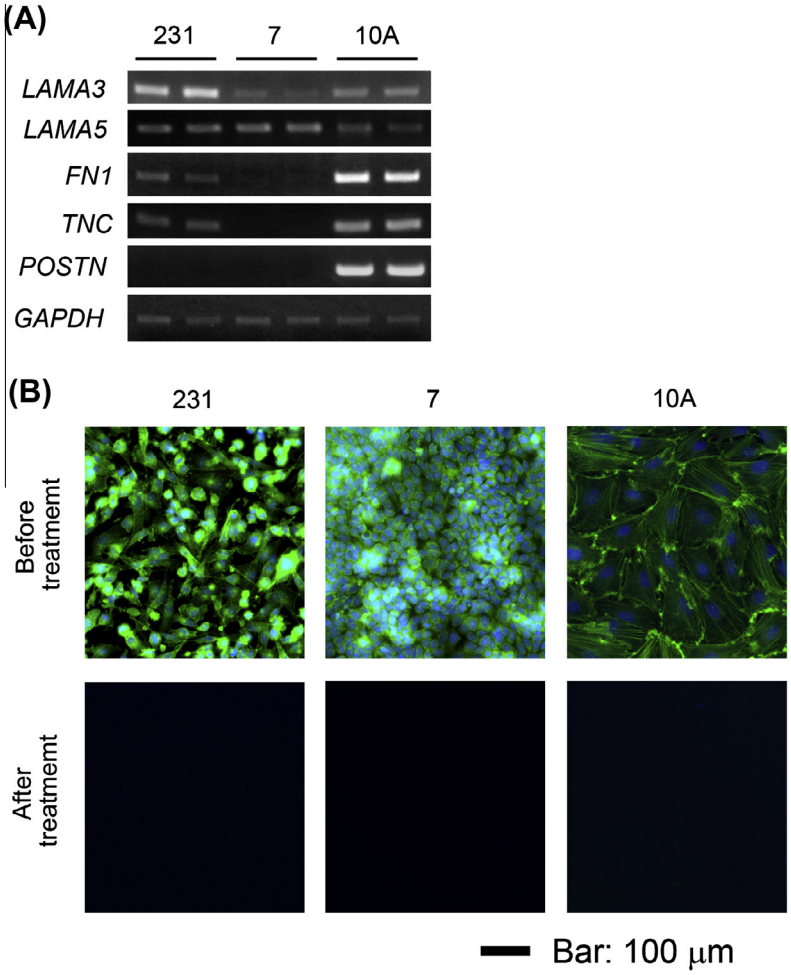

Fig. 1. Preparation of staged tumorigenesis-mimicking matrices. (A) ECM gene expression patterns in MDA-MB-231, MCF-7, and MCF-10A cells. (B) The removal of cellular components from the staged tumorigenesis-mimicking matrices was confirmed by cell nuclei and actin staining. Cell nuclei and actin were stained in the samples before and after decellularization. Blue pseudo-color and green pseudo-color indicate the cell nuclei and actin, respectively. Bar indicates 100 μm. 231, 7, and 10A indicate MDA-MB-231, MCF-7, and MCF-10A cells, respectively. (For interpretation of the reference to color in this figure legend, the reader is referred to the web version of this article.)

components from the culture by decellularization treatment after 7 days culture. To confirm the decellularization, we observed the remaining actin fibers and cell nuclei (Fig. 1B). Before the decellularization treatment, actin fibers and cell nuclei were evident, while no cell nuclei and actin fibers were observed after the decellularization treatment. These results indicate that the cellular components were completely removed from the matrices. Finally, we checked whether the ECM proteins remained after the decellularization treatment. Whole protein staining with CBB revealed that the ECM proteins remained in the samples, indicating that the staged tumorigenesis-mimicking matrices were prepared successfully (Fig. S1).

3.3. Cell attachment on staged tumorigenesis-mimicking matrices

Next, we evaluated the cell attachment to the staged tumorigenesis-mimicking matrices in a cell attachment assay under serum-free conditions (Fig. 2). All of the cell lines showed poor attachment to bovine serum albumin (BSA)-coated substrates as a negative control, whereas the cells attached well to a bovine fibronectin (FN)-coated substrate and bare TCPS. The numbers of attached cells on the staged tumorigenesis-mimicking matrices were significantly higher than on the BSA-coated substrate, indicating that the staged tumor-mimicking matrices possess cell attachment activities. Comparing among the staged tumorigenesis-mimicking matrices, the attachment activities on the matrices derived from MDA-MB-231 and MCF-7 cancerous cells were significantly lower than the attachment activity on the matrices derived from MCF-10A cells.

3.4. Cell proliferation on staged tumorigenesis-mimicking matrices

To further investigate the cellular functions, we examined cell proliferation on staged tumorigenesis-mimicking matrices (Fig. 3A–C). The proliferation of MDA-MB-231 and MCF-7 cancer cells was promoted on only the matrices derived from MDA-MB-231 cancerous cells (Fig. 3A and B). These results suggest that the cancer cells require cancerous ECM for their proliferation, and the ECM in benign/normal tissue suppresses cancer cell proliferation to maintain tissue homeostasis. On the other hand, MCF-10A cell proliferation was promoted only on the matrices derived from the MCF-10A cells (Fig. 3C). MDA-MB-231 cells highly expressed *LAMA3* and *LAMA5*, which are composed of laminin-332 and laminin-511/521, respectively. These laminins strongly activate the phosphatidylinositol 3-kinase (PI3K)/Akt pathway, which promotes breast cancer cell proliferation [22,23]. Therefore, it appears that the proliferation of MDA-MB-231 and MCF-7 cancer cells is promoted by the presence of these laminins in the matrices derived from MDA-MB-231 cells. On the other hand, the proliferation of MCF-10A cells was promoted on the matrices derived from MCF-10A cells. MCF-10A cells highly expressed *TNC*, which promotes MCF-10A cell proliferation [24]. Therefore, it appears that the proliferation of MCF-10A cells was promoted by tenascin-C in the matrices derived from MCF-10A cells.

3.5. Chemoresistance of MDA-MB-231 cells on staged tumorigenesis-mimicking matrices

Finally, we compared the cytotoxicity of the anti-cancer drugs, 5-fluorouracil (5-FU) and doxorubicin (Dox), against MDA-MB-231 cells on the staged tumorigenesis-mimicking matrices. The cytotoxicity of 5-FU against MDA-MB-231 cells significantly decreased on matrices derived from MDA-MB-231 cells (Fig. 3D). However, the cytotoxicity of Dox against MDA-MB-231 cells was not affected by the matrices (Fig. 3E). It has been reported that the ECM plays important roles in the chemoresistance of cancer cells [25]. In

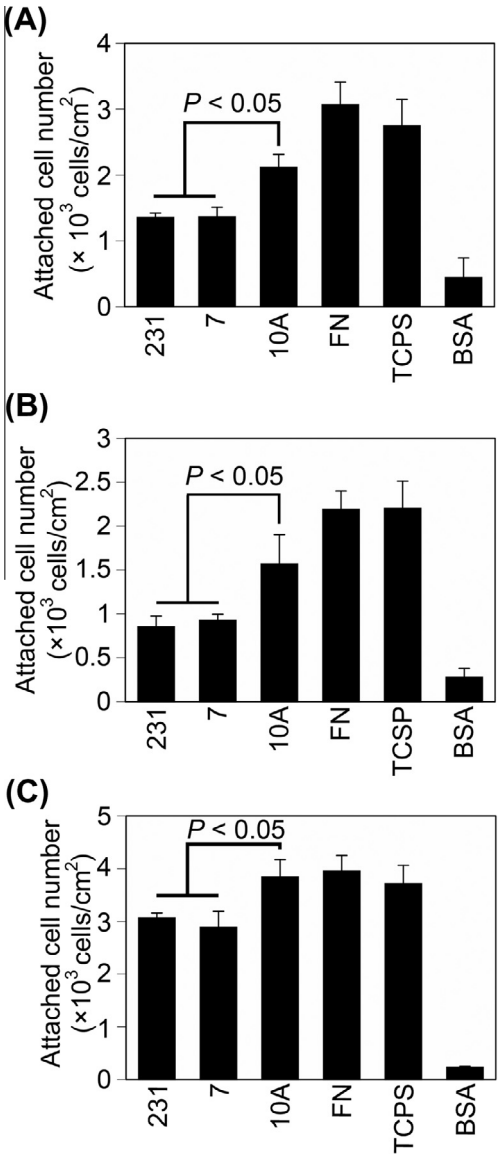

Fig. 2. The attachment of (A) MDA-MB-231, (B) MCF-7, and (C) MCF-10A cells on staged tumorigenesis-mimicking matrices. 231, 7, and 10A indicate the matrices derived from MDA-MB-231, MCF-7, and MCF-10A cells, respectively. Data represent the means ± SD ($n = 3$).

our study, we showed that inhibitory effect of the ECM on the cytotoxicity of 5-FU was dependent on the types of staged tumorigenesis-mimicking matrices (Fig. 3D). Proliferation of MDA-MB-231 cells was promoted on the matrices derived from MDA-MB-231 cells, indicating that cell proliferation signaling pathways, such as the PI3K/Akt pathway, were strongly activated. Such intracellular signals can protect cancer cells from drug-induced apoptosis [25]. Therefore, it might be possible that the cytotoxicity of 5-FU against MDA-MB-231 cells was inhibited on the matrices derived from MDA-MB-231 cells by strong activation of the cell proliferation signaling pathways. Additionally, we cannot exclude the possibility that the activity of drug efflux transporters is increased on the matrices to suppress the cytotoxicity of 5-FU.

In contrast to 5-FU, the matrices had little effect on the cytotoxicity of Dox (Fig. 3D). Although the ECM plays important roles in the chemoresistance of cancer cells, our results suggest that the effect of the ECM on the chemoresistance of cancer cells was dependent on the types of anti-cancer drugs, which is consistent with previous reports [26]. Additionally, several reports showed that

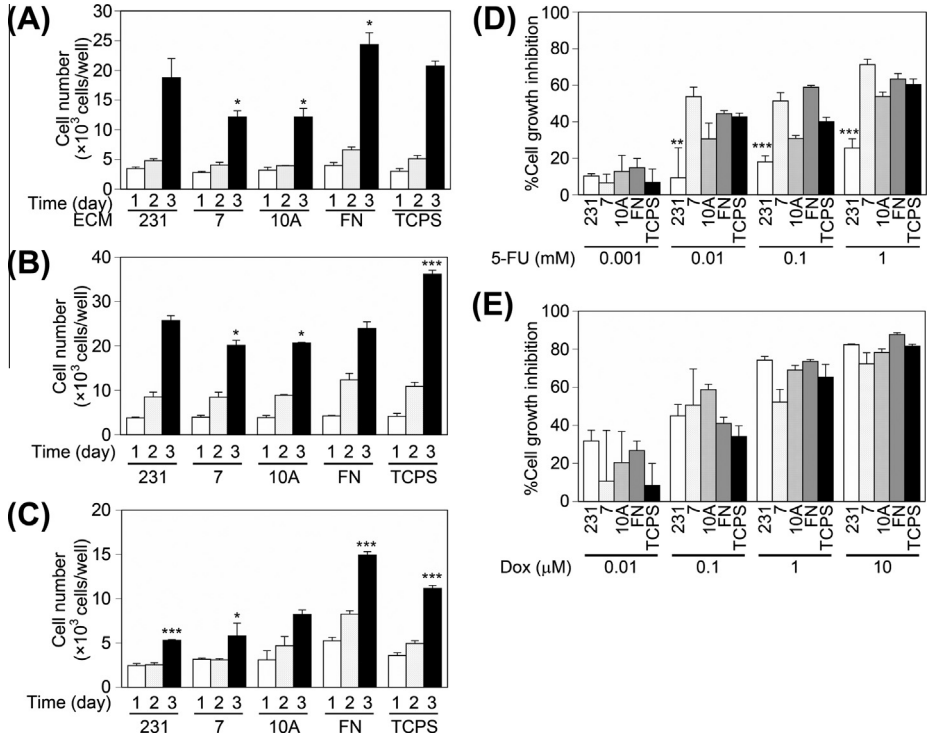

Fig. 3. Cell proliferation and chemoresistance on staged tumorigenesis-mimicking matrices. The proliferation of (A) MDA-MB-231, (B) MCF-7, and (C) MCF-10A cells on staged tumorigenesis-mimicking matrices. 231, 7, and 10A indicate the matrices derived from MDA-MB-231, MCF-7, and MCF-10A cells, respectively. Data represent the means ± SD ($n = 3$). $^{*}P < 0.05$ and $^{***}P < 0.005$ *vs.* 231 in Fig. 3A and 3B. $^{*}P < 0.05$ and $^{***}P < 0.005$ *vs.* 10A in Fig. 3C. Cytotoxicity of (D) 5-FU and (E) Dox against MDA-MB-231 cells on staged tumorigenesis-mimicking matrices. Data represent the means ± SD ($n = 3$). $^{**}P < 0.01$ and $^{***}P < 0.005$ *vs.* other matrices.

cell-derived decellularized matrices can enhance the chemoresistance against anti-cancer drugs. However, our results indicate that not all cell-derived matrices can enhance the chemoresistance of cancer cells. Cell sources for matrix preparation to enhance chemoresistance should be considered. The malignancy of cancer cells may be an important consideration in this regard.

MCF-10A cells have been well used as a normal breast cell model. In this study, we expected that MCF-10A cells could be applied for the preparation of a normal breast tissue ECM model. However, comparing the ECM gene expression patterns, MCF-10A cells showed the characteristics of fibrocystic disease. Therefore, normal human mammary epithelial cells should be applied for the preparation of a normal breast tissue ECM model as one of the staged tumorigenesis-mimicking matrices in the future.

In this study, we prepared three types of staged tumorigenesis-mimicking matrices derived from MDA-MB-231, MCF-7, and MCF-10A cells. Additionally, we examined cell functions, such as cell attachment, proliferation, and chemoresistance against anti-cancer drugs. A previous study examined cancer cell functions on matrices derived from normal and malignant fibroblasts, but not cancer cells at different malignant stages. Our report is the first trial that examined cancer cell functions on the matrices derived from cells at different malignant stages. Our results showed that cancer and normal/benign cells presented different behaviors on staged tumorigenesis-mimicking matrices according to the types of cells used for the matrix preparation (Table S2). Therefore, staged tumorigenesis-mimicking matrices might be useful *in vitro* ECM models to investigate the roles of ECM in tumor progression.

Acknowledgments

This work was supported by the Funding Program for Next Generation World-Leading Researchers (NEXT Program) from the Ministry of Education, Culture, Sports, Science and Technology (MEXT), Japan. T. Hoshiba was also supported in part by a Grant-in-Aid for Challenging Exploratory Research (24659867) from MEXT, Japan.

Appendix A. Supplementary data

Supplementary data associated with this article can be found, in the online version, at http://dx.doi.org/10.1016/j.bbrc.2013.08.038.

References

[1] D. Hanahan, R.A. Weinberg, The hallmarks of cancer, Cell 100 (2000) 57–70.
[2] D. Hanahan, R.A. Weinberg, Hallmarks of cancer: the next generation, Cell 144 (2011) 646–674.
[3] I.P. Witz, Yin-Yang, Activities and Vicious Cycles in the Tumor Microenvironment, Cancer Res. 68 (2008) 9–13.
[4] E. Ioachim, A. Charchanti, E. Briasoulis, et al., Immunohistochemical expression of extracellular matrix components tenascin, fibronectin, collagen type IV and laminin in breast cancer: their prognostic value and role in tumour invasion and progression, Eur. J. Cancer 38 (2002) 2362–2370.
[5] R.O. Hynes, The extracellular matrix: not just pretty fibrils, Science 326 (2009) 1216–1219.
[6] G. Kharaishvili, M. Cizkova, K. Bouchalova, et al., Collagen triple helix repeat containing 1 protein, periostin and versican in primary and metastatic breast cancer: an immunohistochemical study, J. Clin. Pathol. 64 (2011) 977–982.
[7] S.-Y. Kwon, S.W. Chae, S.P. Wilczynski, et al., Laminin 322 expression in breast carcinoma, Appl. Immunohistochem. Mol. Morphol. 20 (2012) 159–164.
[8] J. Chia, N. Kusuma, R. Anderson, et al., Evidence for a role of tumor-derved laminin-511 in the metastatic progression of breast cancer, Am. J. Pathol. 170 (2007) 2135–2148.
[9] T. Oskarsoson, S. Acharyya, X.H.-F. Zhang, et al., Breast cancer cells produce tenaschi C as a metastatic niche component to colonize the lungs, Nat. Med. 17 (2011) 867–874.
[10] G.E. Plopper, S.Z. Domanico, V. Cirulli, et al., Migration of breast epithelial cells on laminin-5: differential role of integrins in normal and transformed cell types, Breast Cancer Res. Treat. 51 (1998) 57–69.
[11] T. Hoshiba, T. Yamada, H. Lu, et al., Maintenance of cartilaginous gene expression on extracellular matrix derived from serially passaged chondrocytes during *in vitro* chondrocyte expansion, J. Biomed. Mater. Res. Part A 100 (2012) 694–702.
[12] T. Hoshiba, H. Lu, N. Kawazoe, et al., Decellularized matrices for tissue engineering, Expert Opin. Biol. Ther. 10 (2010) 1717–1728.

[13] T. Hoshiba, N. Kawazoe, T. Tateishi, et al., Development of stepwise osteogenesis-mimicking matrices for the regulation of mesenchymal stem cell functions, J. Biol. Chem. 284 (2009) 31164–31173.
[14] T. Hoshiba, N. Kawazoe, T. Tateishi, et al., Development of extracellular matrices mimicking stepwise adipogenesis of mesenchymal stem cells, Adv. Mater. 22 (2010) 3042–3047.
[15] T. Hoshiba, N. Kawazoe, G. Chen, Mechanism of regulation of pparg expression of mesenchymal stem cells by osteogenesis-mimicking extracellular matrices, Biosci. Biotechnol. Biochem. 75 (2011) 2099–2104.
[16] T. Hoshiba, N. Kawazoe, G. Chen, The balance of osteogenic and adipogenic differentiation in human mesenchymal stem cells by matrices that mimic stepwise tissue development, Biomaterials 33 (2012) 2025–2031.
[17] R. Tuli, S. Tuli, S. Nandi, Transforming growth factor-β-mediated chondrogenesis of human mesenchymal progenitor cells involves N-cadherin and mitogen-activated protein kinase and Wnt signaling cross-talk, J. Biol. Chem. 278 (2003) 41227–41236.
[18] A.C. Hielscher, C. Qiu, S. Gerecht, Breast cancer cell-derived matrix supports vascular morphogenesis, Am. J. Physiol. Cell Physiol. 302 (2012) C1243–C1256.
[19] H.D. Soule, T.M. Maloney, S.R. Wolman, et al., Isolation and characterization of a spontaneously immortalized human breast epithelial cell line, MCF-10, Cancer Res. 50 (1990) 6075–6086.
[20] A.A. Howeedy, I. Virtanen, L. Laitnen, et al., Differential distribution of tenascin in the normal, hyperplastic, and neoplastic breast, Lab. Invest. 63 (1990) 798–806.
[21] H. Yoshimura, M. Michishita, K. Ohkusu-Tsukada, et al., Increased presence of stromal myofibroblasts and tenascin-C with malignant progression in canine mammary tumors, Vet. Pathol. 48 (2011) 313–321.
[22] J. Gu, A. Fujibayashi, K.M. Yamada, et al., Laminin-10/11 and fibronectin differentially prevent apoptosis induced by serum removal via phosphatidylinositol 3-kinase/Akt- and MEK1/ERK-dependent pathways, J. Biol. Chem. 277 (2002) 19922–19928.
[23] M.C. Bertucci, C.A. Mitchell, Phosphoinositide 3-kinase and INPP4B in human breast cancer, Ann. N.Y. Acad. Sci. 1280 (2013) 1–5.
[24] A. Taraseviciute, B.T. Vincent, P. Schedin, et al., Quantitative analysis of three-dimensional human mammary epithelial tissue architecture reveals a role for tenascin-C in regulating c-met function, Am. J. Pathol. 176 (2010) 827–838.
[25] F. Aoudjit, K. Vuori, K, Integrin signaling in cancer cell survival and chemoresistance, Chemother. Res. Pract. 25 (2010) 90–92, http://dx.doi.org/10.1155/2012/283181.
[26] I. Serebriiskii, R. Castelló-Cros, A. Lamb, et al., Fibroblast-derived 3D matrix differentially regulates the growth and drug-responsiveness of human cancer cells, Matrix Biol. 27 (2008) 573–585.